Pergamon

PII: S0968-4328(97)00050-4

Micron Vol. 28, No. 6, pp. 419–431, 1997

0968-4328/97 $17.00+0.00

High Resolution Microanalysis and Three-Dimensional Nucleosome Structure Associated with Transcribing Chromatin

GREGORY J. CZARNOTA,* DAVID P. BAZETT-JONES,† ELIZABETH MENDEZ,‡¶
VINCENT G. ALLFREY‡ and F. PETER OTTENSMEYER*§

*Department of Medical Biophysics, University of Toronto and Division of Molecular and Structural Biology, Ontario Cancer Institute, 610 University Avenue, Toronto, ON, Canada M5G 2M9
†Departments of Anatomy and Medical Biochemistry, The University of Calgary, Calgary, AB, Canada T2N 4N1
‡Laboratory of Cell Biology, Rockefeller University, New York, NY 10021, U.S.A.

(*Received* 2 *May* 1997; *accepted* 7 *August* 1997)

Abstract—The nucleosome is the ubiquitous and fundamental DNA–protein complex of the eukaryotic chromosome, participating in the packaging of DNA and in the regulation of gene expression. Biophysical studies have implicated changes in nucleosome structure from chromatin that is quiescent to active in transcription. Since DNA within the nucleosome contains a high concentration of phosphorus whereas histone proteins do not, the nucleosome structure is amenable to microanalytical electron energy loss mapping of phosphorus to delineate the DNA within the protein–nucleic acid particle.Nucleosomes associated with transcriptionally active genes were separated from nucleosomes associated with quiescent genes using mercury-affinity chromatography. The three-dimensional image reconstruction methods for the total nucleosome structure and for the 3D DNA–phosphorus distribution combined quaternion-assisted angular reconstitution of sets of single particles at random orientations and electron spectroscopic imaging. The structure of the active nucleosome has the conformation of an open clam-shell, C- or U-shaped in one view, elongated in another, and exhibits a protein asymmetry. A three-dimensional phosphorus map reveals a conformational change in nucleosomal DNA compared to DNA in the canonical nucleosome structure. It indicates an altered superhelicity and is consistent with unfolding of the particle. The results address conformational changes of the nucleosome and provide a direct structural linkage to biochemical and physiological changes which parallel gene expression. © 1997 Elsevier Science Ltd. All rights reserved

Key words: nucleosomes, gene expression, chromatin, electron microscopy, electron spectroscopic imaging, microanalysis, three-dimensional reconstruction.

INTRODUCTION

The nucleosome is a eukaryotic nucleoprotein complex composed of DNA wrapped about a histone protein core. It is the primary DNA packaging unit in the chromosome and is also involved in the facilitation, modulation and repression of gene expression (reviewed in van Holde, 1988; Turner, 1991; Felsenfeld, 1992; Grunstein *et al.*, 1992; Wolffe, 1994). Its structure is recognized to be dynamic *in vitro*, as inferred by a number of physicochemical studies which indicate changes in nucleosome structure in response to pH, ionic environment and post-translational modifications (reviewed in van Holde, 1988).

A number of studies have addressed changes in nucleosome structure associated with gene expression (reviewed in van Holde *et al.*, 1992). Crystallographic investigations of nucleosome particles using X-ray and neutron diffraction (Bentley *et al.*, 1984; Richmond *et al.*, 1984; Uberbacher and Bunick, 1989; Struck *et al.*, 1992; Arents and Moudrianakis, 1993) and electron microscopic studies in conjunction with three-dimensional image reconstruction (Czarnota and Ottensmeyer, 1996) have shown that the structure of the nucleosome from transcriptionally quiescent genes is consistent with that of a compact oblate ellipsoid under some ionic conditions. In contrast, elongated particles (Locklear *et al.*, 1990; Oliva *et al.*, 1990) and so-called lexosome forms of the particle (Prior *et al.*, 1984) have been detected by electron microscopy and have been associated with transcriptional activity. Changes in nucleosome structure have been associated with gene expression in investigations of the effects of post-translational modifications such as the acetylation of constituent histone proteins (reviewed in Oliva *et al.*, 1987; Locklear *et al.*, 1990). These studies have found significant differences in characteristics such as thermal denaturation, nuclease sensitivity (Simpson, 1978; Ausio and van Holde, 1986) and electrophoretic mobility (Imai *et al.*, 1986) in comparison to hypoacetylated nucleosomes, and have also indicated loosened histone–DNA contacts in hyperacetylated particles (Oliva *et al.*, 1987; Locklear *et al.*, 1990). Altered nucleosome shapes have been observed for hyperacetylated particles (Bode, 1984; Bode *et al.*, 1980, 1983; Bertrand *et al.*, 1984; Bazett-Jones *et al.*, 1996) and have been inferred from a

¶Present address: Department of Embryology. Carnegie Institute of Washington, 115 W. University Parkway, Baltimore, MD 21210-3399, U.S.A.
§Corresponding author. Tel: (416) 946-2969; fax: (416) 946-6529; email: fpo@oci.utoronto.ca

decrease in the number of turns of nucleosomal DNA around the particle's central axis (Bauer *et al.*, 1994).

Mercury-affinity chromatography permits the isolation of nucleosome particles which are specific for actively transcribing chromatin (Allegra *et al.*, 1987; Chen *et al.*, 1987, 1990; Walker *et al.*, 1990). Upon the activation of gene expression, nucleosomal sulphydryls on histone H3, which are otherwise buried within the protein core of the particle, become accessible to chemical agents. Nucleosomes with such accessible sulphydryls can bind to mercury-conjugated chromatographic agarose in temporal and physiological relation to the period of gene expression. This purification approach (Allegra *et al.*, 1987; Chen *et al.*, 1987, 1990; Walker *et al.*, 1990), coupled with electron spectroscopic imaging (ESI) and with the 3D reconstruction methods used in previous preliminary structural investigations (Bazett-Jones *et al.*, 1996; Czarnota and Ottensmeyer, 1996; Farrow and Ottensmeyer, 1992, 1993; Czarnota *et al.*, 1994), forms the basis for this study of nucleosome structure in association with gene expression, and of the three-dimensional DNA phosphorus distribution within the particle.

Electron spectroscopic imaging permits structural studies at moderately high resolution to be carried out simultaneously with elemental microanalysis. It is particularly suited for use in the study of nucleoprotein complexes such as the nucleosome, since it permits the direct identification and mapping of the nucleic-acid phosphorus distribution; hence the DNA trajectory in the nucleosome particles can be determined at the same time and from the same data used for the structure determination of the entire particle (Adamson-Sharpe and Ottensmeyer, 1981; Bazett-Jones and Ottensmeyer, 1981; Harauz and Ottensmeyer, 1984a). The approach has been used previously in two-dimensional mapping to investigate numerous nucleoprotein complexes including ribosomes, transcription factors such as UBF and TFIIIA bound to promoter DNA (Bazett-Jones and Brown, 1989; Bazett-Jones *et al.*, 1994; Neil *et al.*, 1996), and nucleosomes in different ionic environments (Harauz and Ottensmeyer, 1984a; Locklear *et al.*, 1990; Oliva *et al.*, 1990; Bazett-Jones *et al.*, 1996; Czarnota and Ottensmeyer, 1996). Although the technique requires a higher exposure of the specimen to the electron beam than non-microanalytical microscopic methods, the stability of DNA–protein complexes permits two-dimensional image-based analyses at moderately high resolutions (Adamson-Sharpe and Ottensmeyer, 1981; Bazett-Jones and Ottensmeyer, 1981; Harauz and Ottensmeyer, 1984a; Bazett-Jones and Brown, 1989; Bazett-Jones *et al.*, 1994; Neil *et al.*, 1996). The technique has a very high sensitivity, easily capable of detecting the 300 P atoms in a single nucleosome, with a lower limit of 30 atoms at a signal-to-noise ratio of 5 that is considered the threshold of certain detectability (Adamson-Sharpe and Ottensmeyer, 1981). Except for X-ray diffraction, when crystals can be obtained, other high-resolution approaches that can provide simultaneous structural and elemental information on nucleosome particles are currently not available.

Computational reconstruction methods now permit the use of electron micrographs of sets of single particles at random orientations to determine a three-dimensional structure for any particular macromolecule or macromolecular complex being studied (Vainshtein and Goncharov, 1986; van Heel, 1987; Farrow and Ottensmeyer, 1992, 1993; Beniac *et al.*, 1997a, 1997b, 1997c). Our approach is based on the principle of angular reconstitution (Vainshtein and Goncharov, 1986; van Heel, 1987; Beniac *et al.*, 1997a) and relies on quaternion mathematics (Harauz, 1990) to optimize the 3D fit amongst electron microscopic images of many differently oriented biological macromolecules. The quaternion-assisted angular reconstitution approach has been tested on simulated images (Farrow and Ottensmeyer, 1992, 1993) and used previously in the investigation of the structure of a number of other biological macromolecules and complexes including ribosomes (Beniac *et al.*, 1997b), the 54 kDa subunit of mammalian signal recognition particle (Czarnota *et al.*, 1994), the 18 kDa myelin basic protein (Beniac *et al.*, 1997c), the 2.25 MDa phosphoenol–pyruvate synthase (Harauz *et al.*, 1998), and nucleosomes from quiescent genes in different ionic environments (Czarnota and Ottensmeyer, 1996). It is applied here in conjunction with ESI–phosphorus microanalysis to delineate the 3D distribution of DNA in the nucleosome.

Our earlier study on nucleosomes from active genes using two-dimensional image analysis (Bazett-Jones *et al.*, 1996) demonstrated changes in nucleosome conformation as well as changes in the distribution of nucleosomal DNA in two-dimensional projection. The study presented here details the results of a full three-dimensional structural characterization of nucleosome particles, chromatographically purified from chromatin active in transcription, and of the DNA conformation within them. Using three-dimensional image reconstruction methods, we have determined a structure for the nucleosome associated with such chromatin at 32 Å resolution. The structure reveals significant differences in comparison to the canonical conformation of the transcriptionally quiescent nucleosome. The nucleosome associated with transcribing genes has an elongated conformation from one perspective, and in another has an asymmetric mass distribution in the form of a C- or U-shape with an accessible core consistent with physicochemical and biophysical studies. The corresponding three-dimensional phosphorus distribution within the particle indicates that the DNA conformation is consistent with such unfolding of the total nucleosome and can be represented approximately by two turns of a bent spring. Thus both the DNA and the histone arrangement in the particle have an altered conformation compared to the canonical nucleosome.

MATERIALS AND METHODS

Preparation of chromatin

The methods used to purify nucleosomes from transcriptionally active genes have been published in

complete form previously (Allegra *et al.*, 1987; Chen *et al.*, 1987, 1990; Walker *et al.*, 1990; Bazett-Jones *et al.*, 1996). In short, nucleosomes were prepared from human adenocarcinoma cells (COLO 320 DM, ATCC). Particles were released from prepared nuclei by limited digestion with micrococcal nuclease using conditions optimized to minimize degradation of unfolded nucleosome monomers associated with transcriptionally active genes. Particles were chemically fixed in order to preserve their conformations as before (Bazett-Jones *et al.*, 1996) using 1% (w/v) buffered EM-grade formaldehyde for 5 min at room temperature in 50 mM Tris–HCl pH 7.4, 50 mM NaCl, 0.5 mM $MgCl_2$, an effective ionic strength near physiological (Czarnota and Ottensmeyer, 1996), 1 mM β-mercaptoethanol and 5 mM sodium butyrate. More extensive fixation methods incorporating glutaraldehyde in addition to formaldehyde have been devised for nucleosome particles (Zabal *et al.*, 1993). These have been used primarily for preparing particles at extremely high and extremely low non-physiological ionic strengths where nucleosome structure is recognized to be extremely unstable. Additionally, such fixation protocols have been employed in order to prepare particles for critical-point drying where organic solvents such as ethanol and amyl acetate are utilized which might otherwise destabilize the structure of a particle which has not been extensively fixed.

In this study sodium butyrate was added to the cells prior to nucleosome isolation, to inhibit nucleosome deacetylation. Particles were subsequently passed through Sephacryl S-200 (1.5 cm × 50 cm column) to remove any particles associated with non-nucleosomal components having a combined molecular mass greater than 200 kDa.

Nucleosomes associated with transcriptionally active genes were separated from nucleosomes from quiescent chromatin by affinity chromatography using an organomercurial–agarose column. The procedure exploits the fact that nucleosomes associated with transcriptionally active genes exhibit accessible H3 sulphydryls that are otherwise buried in the protein core of the nucleosome (Allegra *et al.*, 1987; Chen *et al.*, 1987, 1990; Walker *et al.*, 1990). The characterization of this separation procedure is described and documented elsewhere (Allegra *et al.*, 1987; Chen *et al.*, 1987, 1990; Walker *et al.*, 1990; Bazett-Jones *et al.*, 1996). The column initially separated nucleosomes into a flow-through fraction containing particles from transcriptionally inactive genes and a bound fraction of particles which contained nucleosomes associated with transcriptionally active genes. The bound particles were compartmentalized into two fractions. Any nucleosome particles adhering to the column non-specifically by association with sulphydryl-containing non-histone proteins were removed by an elution step with 500 mM NaCl. This step has been previously demonstrated not to alter nucleosome structure with the specific conditions used here (Bazett-Jones *et al.*, 1996). The second step was elution of H3–sulphydryl-bound particles by 20 mM dithiothreitol (DTT). Nucleosomes from the flow-through and the DTT-eluted fractions contained stoichiometric quantities of all four histones (Walker *et al.*, 1990); they have been characterized extensively elsewhere (Allegra *et al.*, 1987; Chen *et al.*, 1987, 1990; Walker *et al.*, 1990). Our previous electron microscopic mass analysis using ESI indicated that the flow-through fraction had an average total mass of 208 ± 21 kDa, an average DNA content of 162 ± 28 bp and a protein content of 101 ± 29 kDa. The DTT-eluted nucleosome particles had a mass of 212 ± 29 kDa, an average DNA content of 155 ± 40 bp, and a protein content of 111 ± 28 kDa (Bazett-Jones *et al.*, 1996; n=95). Within the limits of electron microscopic mass analyses the compositions of the flow-through and DTT-eluted particles may be considered identical, as previously detailed (Bazett-Jones *et al.*, 1996). Nucleosome particles from the flow-through and DTT-eluted fractions were subsequently subjected to analysis using electron microscopy and three-dimensional image reconstruction analyses, as described below.

Electron microscopy

Nucleosome particles were analyzed by spectroscopic electron microscopy using a Zeiss EM902 equipped with an imaging electron energy filter. The approach, also referred to as electron spectroscopic imaging (ESI), permits imaging with electrons which have lost a specific amount of energy to obtain elemental maps using inner-shell ionization interactions with particular elements in the specimen (155 ± 8 eV for phosphorus). In nucleoprotein complexes, maps of the phosphorus distribution represent projections of the phosphate backbone of the nucleic acid component. This method has been used previously to investigate the nucleic acid component of nucleosomes, ribosomes, the signal recognition particle, and transcription factors bound in complex with DNA (Bazett-Jones and Ottensmeyer, 1981; Harauz and Ottensmeyer, 1984a; Andrews *et al.*, 1987; Oliva *et al.*, 1990; Bazett-Jones *et al.*, 1994, 1996; Neil *et al.*, 1996). It provides a high-contrast darkfield-like image without the use of ionic-environment-altering heavy atom stains as contrast agents. Low temperature electron microscopy was not used, since our EM902 was not equipped with a cryostage.

Particles were prepared for electron microscopy by applying a 4 μl drop of fixed nucleosomes at a concentration of 20 μg ml^{-1} to 20–30 Å thick glow-discharged carbon support films supported on 1000-mesh copper grids. After 30 s the grids were washed with buffer to remove excess unbound sample, followed by a wash with distilled H_2O. Excess liquid was removed with filter paper, after which the specimen was permitted to air dry. This approach of preparing fixed nucleosome particles has been used previously in our analyses and had been compared with other preparative methods; for chemically fixed particles, results consistent with other drying methods have been observed as well as with quick-freezing and freeze-drying of specimens in vitreous ice (Czarnota, 1995; Czarnota and Ottensmeyer, 1996).

Grids were examined for suitable particle spreads using dose-sparing darkfield-like contrast at an energy loss of 30 eV. Phosphorus-signal-enhanced images were recorded with electrons corresponding to the phosphorus ionization peak at 155 eV energy loss (155 ± 8 eV). A reference image without phosphorus-signal enhancement was recorded subsequently at 120 eV energy loss. Micrographs were recorded on Kodak SO-163 film at a magnification of 13000× or 20000× and were developed in full-strength Kodak D-19 developer for 10 min. At these magnifications the irradiation on the specimen was 375 e Å^{-2} or 900 e Å^{-2}, respectively, with 60% of these doses used for the 155 eV images due to the fall-off in intensity in the energy loss spectrum between 120 and 155 eV. Although these doses are larger than those normally used for imaging, they are virtually the minimum needed for microanalysis. The measured cross-section for phosphorus at 155 eV is 2.4×10^{-20} cm^2 (atom eV)$^{-1}$ (Heng *et al.*, 1990) whereas the cross-section for carbon at 155 eV is calculated to be 6.4×10^{-22} cm^2 (atom eV)$^{-1}$ (Ahn and Krivanek, 1983; Egerton, 1996) and measured by us to be 8.8×10^{-22} cm^2 (atom eV)$^{-1}$. From these values, and also from our experimental measurements, it was found that at a magnification of 20000× the phosphorus signal from a single 100 Å nucleosome on a 25 Å carbon film produces an average signal-to-background ratio of 25% with a signal-to-noise ratio (S/N) between 10 and 20, where an S/N equal to 5 is considered the threshold of certain detectability (Rose, 1973). The high sensitivity of ESI has been previously shown to be readily capable of detecting the 300 P atoms of a single nucleosome at higher doses, with a limit of 30 to 50 P atoms at an S/N of 5 (Bazett-Jones and Ottensmeyer, 1981). Moreover, a spatial resolution of 3–5 Å was measured for the phosphorus signal from the lipid bilayers of murine leukemia viruses (Adamson-Sharpe and Ottensmeyer, 1981). However, at a magnification of 20000× and its corresponding dose the phosphorus signal from about 10 nucleosomes must be averaged to obtain a 20 Å resolution (10 Å pixel) with an S/N=5. In contrast, the signal from the total 100 Å nucleosome itself, including phosphorus and carbonaceous atoms, has an S/N greater than 90 at 155 eV. This latter, stronger signal was used for the determination of the relative orientation angles among the individual nucleosomes (see below).

The electron doses required by this type of microanalytical imaging are nevertheless favourable when compared with other microanalytical approaches; for instance, X-ray microanalysis generally makes use of doses more than one order of magnitude larger at spatial resolutions ten times worse. Typically careful work necessitates doses of 10^4 to 10^5 e Å^{-2} at resolutions of 500 to 2000 Å (LeFurgey *et al.*, 1991; Fiori *et al.*, 1988). One of the best results obtained by the X-ray microanalysis technique are the dot maps for phosphorus and calcium of the sarcoplasmic reticulum, taken in a 24 h exposure with an estimated dose of 10^6 e Å^{-2} at a resolution of 200 Å (Somlyo *et al.*, 1981). Nevertheless, even at doses of only 375 to 900 e Å^{-2}, required here to identify and to localize DNA–phosphorus by microanalytical ESI, it is clear that some fine structural detail will be lost due to radiation-induced structural alterations. This is an inescapable price for obtaining information on the elemental distribution as opposed to purely structural information available at lower doses (e.g., cryoEM at 10 e Å^{-2}). Structural information could have been derived with a lower dose (e.g., using the elastic dark field signal), but the direct relationship between the total structure and the phosphorus distribution within it would have been compromised.

Micrograph pairs (155 eV and 120 eV energy losses) were subsequently aligned and digitized with a pixel size corresponding to 4.8 Å. Automatic particle selection was carried out, based only on integrated particle image intensity which is proportional to molecular weight in ESI images (Czarnota *et al.*, 1994; Bazett-Jones *et al.*, 1996; Czarnota and Ottensmeyer, 1996). Difference images corresponding to phosphorus elemental maps were generated as before (Bazett-Jones *et al.*, 1996).

Two-dimensional image processing

Only particles with a total integrated intensity within one standard deviation of the mean integrated intensity of all 155 eV energy loss particle images were selected for three-dimensional image processing. A similar procedure was subsequently applied using the 120 eV images and the corresponding difference maps, thus further excluding images. Prior to three-dimensional image processing, the signal-to-noise ratio of the 155 eV energy loss particle images was increased by low-pass filtering with a Fourier cut-off at a resolution of 10 Å. The corresponding difference maps were treated similarly except that they were low-pass-filtered to a greater degree since such images are inherently noisier. A resolution of 20 Å was chosen as a limit to the filtering to preserve features of the 20 Å thick DNA trajectory within the nucleosome. The difference maps were thresholded to reduce the noise in images at a value of one standard deviation above the mean background value in the images. This approach has been used before in pretreating sets of difference maps or particle images prior to three-dimensional image reconstruction (Czarnota *et al.*, 1994; Bazett-Jones *et al.*, 1996; Czarnota and Ottensmeyer, 1996). Two-dimensional image processing was carried out in the framework of an antediluvian IMAGIC image processing system (modern version available from Image Sciences Software GMBH, Berlin) using a μVAXII or a VAX Workstation 3100 M38 running VMS 5.4.3 (Digital Equipment Corporation, Maynard, MA, USA).

Three-dimensional image processing

Three-dimensional image processing was carried out as before (Czarnota *et al.*, 1994; Czarnota and Ottensmeyer, 1996), using an approach based on

quaternion-assisted angular reconstitution (Farrow and Ottensmeyer, 1992, 1993). The method permits the three-dimensional reconstruction of biological macromolecules and their complexes from sets of images of both symmetric and asymmetric single particles at random orientations. This process is based on the principle of common lines which states that 2D projection images of a particular 3D macromolecule at different orientations share common lines or axes of integrated (projected) 1D intensity (Vainshtein and Goncharov, 1986; van Heel, 1987; Beniac *et al.*, 1997b). These common lines are determined using sinograms and sinogram correlation functions (van Heel, 1987). The fit among many common lines is then optimized using quaternion mathematics (Harauz, 1990; Farrow and Ottensmeyer, 1992, 1993) to give the relative angular orientations amongst many projection images. This consequently permits the structure of a macromolecule to be reconstructed using algorithms similar to those used in computerized axial tomography (Harauz and Ottensmeyer, 1984b). The method is robust, as tested with simulated images (Farrow and Ottensmeyer, 1992, 1993), and has been used in structural determinations of proteins (Czarnota *et al.*, 1994), ribosomes (Beniac *et al.*, 1997b), enzyme complexes (Harauz *et al.*, 1997) and whole nucleosomes in several different physiological and ionic-strength-dependent conformations (Czarnota and Ottensmeyer, 1996; Bazett-Jones *et al.*, 1996).

Preliminary reconstructions were determined using sets of 75 images of particles from the flow-through nucleosome fraction (transcriptionally quiescent) and from the DTT-eluted nucleosome fraction (associated with transcriptional activity). Further image processing was carried out using images exclusively from the DTT-eluted fraction. In this investigation the number of images used in the initial reconstructions was increased fourfold in order to improve the signal-to-noise ratio of the resulting final reconstruction of the entire DNA–protein complex. The increase in image number was also necessary for elemental microanalysis to permit the calculation of a noise-reduced three-dimensional phosphorus difference map corresponding to the trajectory of nucleosomal DNA. Angular orientations were determined as before, using the strong signal from the 155 eV energy loss images (Czarnota *et al.*, 1994; Czarnota and Ottensmeyer, 1996). This orientation information was used in filtered-back-projection routines (Shepp and Logan, 1974) to reconstruct the complete nucleoprotein complex for the set of 155 eV images which contain both protein and DNA information. The difference images, corresponding to the phosphorus signal only, were subsequently backprojected using the same angular orientations as determined for the corresponding 155 eV energy loss images. This approach was found to be superior in comparison to using the noisier difference images for angular orientation determination, and has been used previously in three-dimensional electron microscopic reconstructions of protein–nucleic acid complexes (Beniac *et al.*, 1997a). In every case the resolution of the 3D reconstruction was not limited by the number of angular orientations of images (van Heel and Harauz, 1986), but by noise in the micrographs and by potential radiation-induced structural alterations from the microanalytical doses required. The actual resolutions of the reconstructions were determined using a Fourier-transform-based phase-residual approach as before (Czarnota *et al.*, 1994; Czarnota and Ottensmeyer, 1996). This method of determining resolution provides a measure of structural identity at particular spatial frequencies and is effectively a consistency measure for the location of features of specific sizes in the reconstructions (Czarnota *et al.*, 1994). In this approach the 300-image set of 155 eV nucleosome images and the corresponding difference maps were split randomly into two sets of images. Reconstructions from each set were determined and then subjected to phase-residual analysis using the entire volume of the reconstruction.

For display purposes, and to compute radii of gyration, reconstructions were low-pass filtered to a resolution with a 60° phase residual (32 Å). Radii of gyration were computed as before (Czarnota and Ottensmeyer, 1996). All computations were carried out on either a μVAXII, a VAX Workstation 3100 M38 or a Silicon Graphics Indigo (Silicon Graphics Inc., Mountain View, CA, USA). Three-dimensional visualization was carried out using the program SGI–Explorer V 2.2.2 on the Silicon Graphics Indigo computer. Thresholds for the visualization of the nucleosome reconstructions and the three-dimensional difference map were set according to the theoretical volume of the combined nucleic acid and protein components of the nucleosome and according to the theoretical volume of nucleosomal DNA, respectively. These thresholds were calculated using a protein density of $1.3\ g\ cm^{-3}$, a DNA density of $1.7\ g\ cm^{-3}$, 155 bp DNA, 620 Da $(bp\ DNA)^{-1}$, and a contribution of 109 kDa from the histone core of the nucleosome (Cantor and Schimmel, 1980; van Holde, 1988).

RESULTS

We present here results of a joint microanalytical and structural investigation that describes the three-dimensional conformation of nucleosomes associated with transcriptional activity and details in three dimensions the differences with respect to particles associated with transcriptional quiescence.

Chromatographically purified nucleosome particles associated with transcriptionally active genes and imaged using electron spectroscopic microscopy are shown in Fig. 1. The particles exhibited a U- or C-shaped appearance in one profile with a height of approximately 110 Å and a cleft extending approximately 45 Å towards the centre of the particle. They appeared elongated in other profiles, with lengths near 125 Å. By two-dimensional analysis a mass asymmetry has been characterized in such images, with one pseudo-twofold symmetric domain of the nucleosome containing approximately 15% more mass than the other

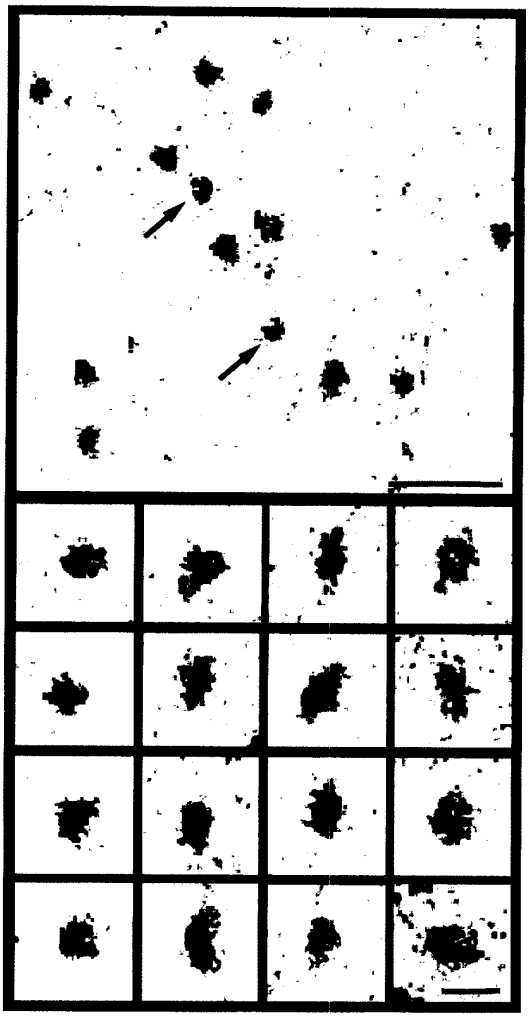

Fig. 1. Images of representative structures of unfolded nucleosomes associated with active transcribing chromatin. These particles were eluted with DTT and appear elongated in some profiles and C-shaped in other profiles. Representative C-shaped particles are indicated by arrows. Upper and lower scale bars indicate 500 Å and 100 Å, respectively.

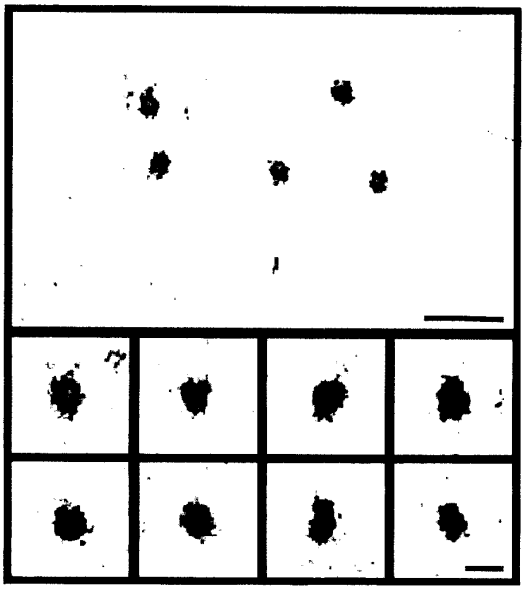

Fig. 2. Images of transcriptionally inactive nucleosomes. The particles were part of the flow-through fraction and predominantly appear with disc-like profiles (diameter=110 Å). Other 'edge-on' views are also represented (length=110 Å, width=65 Å). Upper and lower scale bars indicate 500 Å and 100 Å, respectively.

(Bazett-Jones *et al.*, 1996). This open structure was not the result of irradiation with the microanalytical doses used, which are higher than those necessary merely for imaging. As a control, nucleosome particles associated with transcriptionally quiescent chromatin imaged at the same dose exhibited a canonical nucleosome conformation (Fig. 2). Such particles had predominantly circular profiles, consistent with a disc-like conformation, though rarer and thinner edge-on views were also evident. As previously detailed, no mass asymmetry was apparent in these images. For the purposes of three-dimensional image reconstruction, image classification methods were used as before (Czarnota and Ottensmeyer, 1996) with both types of particles in order to ensure that no single view was under-represented in each set of images.

In order to determine the gross conformations of the two nucleosome types, three-dimensional reconstructions (Fig. 3) were calculated using sets of 75 images each of nucleosomes from the corresponding fractions by a quaternion-assisted angular reconstitution approach. The reconstruction of the nucleosomes from the DTT-eluted fraction associated with transcriptionally active genes was C-shaped in one profile and elongated at a perpendicular orientation. The handedness of the reconstruction, which was not discernable from the 3D structure, was established subsequently from the constituent DNA by the reconstruction of a three-dimensional difference map. The reconstruction of the transcriptionally inactive flow-through nucleosome fraction yielded a conformation generally consistent with the canonical structure of the nucleosome (Bentley *et al.*, 1984; Richmond *et al.*, 1984; Uberbacher and Bunick, 1989; Struck *et al.*, 1992; Arents and Moudrianakis, 1993). In one orientation the reconstruction presented a circular profile with a diameter of 110 Å. The side view presented a thinner profile, 110 Å in length and with a height 10 Å greater than the 57 Å height of the crystallographic form of the nucleosome. This conformation is consistent with a previous three-dimensional reconstruction of nucleosomes from transcriptionally quiescent genes, and may represent the differences between the crystallographic conditions and the ionic environment used in this study (Czarnota and Ottensmeyer, 1996). Exposure of this fraction of nucleosomes to 500 mM NaCl did not change their conformation (Bazett-Jones *et al.*, 1996), indicating that the C-shape of the DTT-eluted chromatographic fraction is an intrinsic structure and not a result of the chromatographic ionic conditions to which the

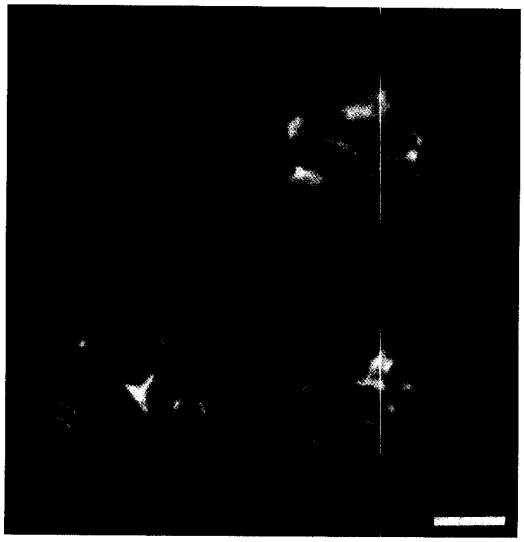

Fig. 3. Preliminary three-dimensional reconstructions. Preliminary reconstructions for the DTT-eluted (top) and the flow-through fraction (bottom) nucleosomes are shown. In the images of the DTT-eluted nucleosome reconstruction the left view is related to the right by a 90° rotation towards the left about a vertical axis in the plane of the page. In the images of the flow-through fraction reconstruction the left view is related to the right by a rotation about a horizontal axis in the plane of the page such that the bottom edge of the nucleosome in the right view faces forward in the left view. Nucleosome reconstructions are shown at a threshold which corresponds to the theoretical volume of the combined protein and nucleic acid components of the particle. The scale bar indicates 50 Å.

chemically fixed nucleosomes are exposed during their separation (Bazett-Jones *et al.*, 1996).

A three-dimensional reconstruction of particles eluted from the chromatographic material with 500 mM NaCl was not calculated here, since our previous analyses have shown that such nucleosomes are associated with a variety of different proteins such as HMG-1, HMG-2, and acetyltransferases.

Further structural investigations focused on particles from actively transcribing chromatin, since the structure of the transcriptionally quiescent nucleosome is already well characterized by methods including high-resolution crystallography (Bentley *et al.*, 1984; Richmond *et al.*, 1984; Uberbacher and Bunick, 1989; Struck *et al.*, 1992; Arents and Moudrianakis, 1993). Moreover, since difference images are inherently noisier than the corresponding macromolecular images, the image set of nucleosomes associated with transcriptionally active chromatin was expanded to 300 images, a number sufficient to provide interpretable 3D phosphorus maps of nucleoprotein complexes (van Heel and Harauz, 1986).

Figure 4 shows representative difference maps and the corresponding nucleosome images for particles purified using a chromatographic DTT elution. In some views the difference maps, which represent the DNA–phosphorus distribution, exhibited a C-shape in projection similar to a number of views of the entire particle. Some projection difference maps presented two major lobes of phosphorus signal joined at one side; others appeared S-shaped as before (Bazett-Jones *et al.*, 1996). The DNA–phosphorus difference maps are on average similar to the corresponding 155 eV images, as is expected since the DNA moiety of a nucleosome comprises 50% of the particle's mass. From their relative scattering cross-sections at 155 eV, the net signal from the phosphorus atoms in the nucleosome compared to that from the carbonaceous atoms in the particle is in the ratio of 5:3, consistent with the prominence of the net phosphorus signal.

The quaternion-based angular reconstitution approach was utilized in order to calculate angular orientations for each of the 300 individual images of the entire nucleosome particle from the DTT-eluted fraction (Fig. 5) and to determine a three-dimensional reconstruction for these particles (Fig. 6). The same calculated angular orientations were then used to construct a three-dimensional difference map from the corresponding individual difference images (Fig. 6). This represents the 3D DNA–phosphorus trajectory through the nucleosome particle.

A resolution analysis was carried out by splitting the 300-image reconstruction into two 150-image reconstructions (Czarnota *et al.*, 1994). The phase-residual analysis, a measure of structural consistency between the two reconstructions, indicated a resolution of 32 Å at a conservative cut-off of 60° and a value of 21 Å at a cut-off of 90°, a resolution level above which there is no longer any fine-structural similarity. The dispersion of the angular orientations was relatively uniform (Fig. 5), indicating that the resulting resolution of the 3D reconstructions was isotropic throughout.

As anticipated on the basis of our preliminary structures from smaller numbers of nucleosome images, the reconstruction of the set of 300 nucleosomes from the DTT-eluted Hg-column-bound fraction (Fig. 6) was again C-shaped. It exhibited a 40 Å deep groove which extended in towards its centre. The 3D structure had an asymmetric mass distribution in which the mass ratio of its upper domain (Fig. 6) to its lower domain was 36:64, an asymmetry of approximately 15% of the total nucleosome mass. Since there was no mass asymmetry in the 3D phosphorus map (discussed below), the observed asymmetry is protein based. This mass asymmetry is consistent with the relocation of the approximate total mass of two histones, although the resolution of the reconstruction is too low to reveal which histones.

This reconstruction had a calculated radius of gyration of 40.7 Å, similar to the value of 40.5 Å for its 75-image counterpart. Nucleosome particles purified from transcriptionally quiescent chromatin had a radius of gyration of 39.6 Å, indicative of a more compact form.

The corresponding three-dimensional net phosphorus distribution at 32 Å resolution depicts two main lobes of phosphorus signal joined by a more slender linker. No mass asymmetry was observed in this structure. Each lobe had approximately the same volume, and both account for approximately 95% of the volume of the three-dimensional difference map. The bend angle

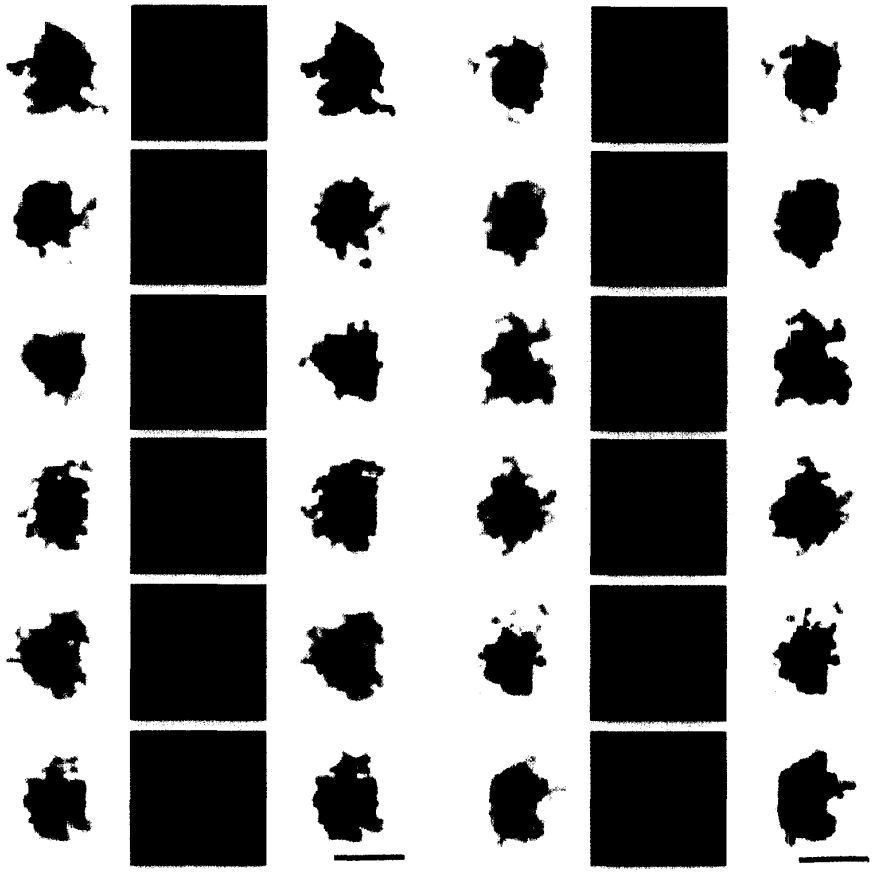

Fig. 4. Electron spectroscopic images of nucleosomes associated with actively transcribing chromatin. In the right and left image-triads the leftmost column of images consists of phosphorus contrast-enhanced nucleosome images obtained at an energy loss of 155 eV. Subtraction of a 120 eV energy loss reference image (not shown) after a background normalization procedure results in the centre column of difference images, interpreted as an elemental map of nucleosomal DNA phosphorus. The right column of images in each set of image triads is an overlay of the difference images on top of the corresponding 155 eV energy loss images. Scale bars indicate 100 Å.

between the two lobes was approximately 30°. Additionally, virtually all of the exterior surface of the volume of this three-dimensional difference map lay within 5–10 Å of the surface of the 155 eV energy loss nucleosome reconstruction and in some places extended no more than 3–5 Å beyond it. A more detailed examination of this phosphorus map in combination with different weighted-backprojection schemes indicated dimples of lesser density in the approximate centre of each lobe when viewed from the top of each lobe (not shown). This suggested that each lobe corresponded to a distorted loop of DNA. An interpretation of this difference map is given in Fig. 7 and discussed below.

DISCUSSION

The nucleosome, the fundamental subunit of chromatin structure, in principle represents a repressive barrier to the transcription of genes. Changes in the structure of the particle have long been suspected to be involved in transforming quiescent chromatin into a transcriptionally active state (van Holde, 1988; Turner, 1991; Felsenfeld, 1992; Grunstein *et al.*, 1992; Wolffe, 1994). This study makes use of a combination of three powerful approaches:

(1) a chromatographic purification of nucleosomes from transcriptionally active chromatin, based on the observation that nucleosomes on actively transcribing genes have exposed sulphydryls which are otherwise buried within the protein core of the particle (Allegra *et al.*, 1987; Chen *et al.*, 1987, 1990; Walker *et al.*, 1990; Arents and Moudrianakis, 1993);

(2) microanalysis by electron spectroscopic imaging, which permits elemental mapping simultaneously with structural imaging; and

(3) three-dimensional reconstruction using quaternion-assisted angular reconstitution, which permits the use of electron micrographs of sets of particles at random unknown orientations.

Fixation and preparation conditions for electron microscopy chosen for this study were identical to those which had previously resulted in consistent canonical oblate, prolate and spheroidal forms from transcription-

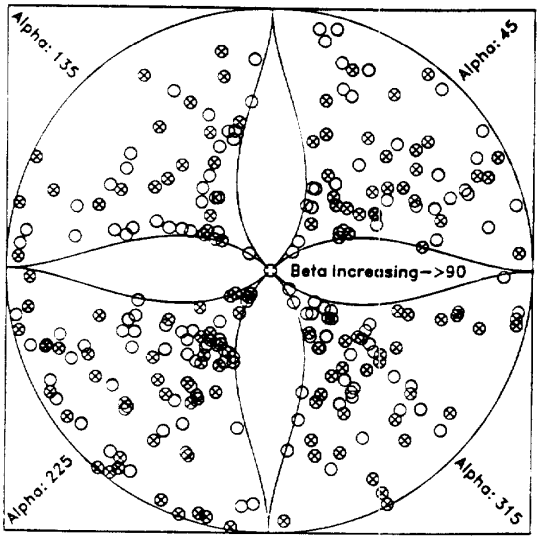

Fig. 5. Calculated molecular orientations for the 300-image reconstruction of the nucleosome associated with transcriptionally active genes. The first two (α, β) of three Euler angles for each image are shown in a cartographic representation of points on the surface of a sphere. These two Euler angles primarily show the inter-image angular relationship. Open circles represent orientations on the top half of the sphere (Euler angle $\beta \leq 90°$). Circles with crosses represent orientations on the bottom half (Euler angle $\beta > 90°$). The third Euler angle, γ, is not shown as it represents a rotation of an image in its own plane. The distribution is relatively uniform.

ally inactive core particle nucleosome preparations (Czarnota and Ottensmeyer, 1996). The C-shaped and asymmetric three-dimensional structure reconstructed for the nucleosome particle associated with actively transcribing chromatin is specific and different from the core particle conformation, but is certainly consistent with the generally altered nucleosome configurations derived from other studies (Prior *et al.*, 1984; Allegra *et al.*, 1987; Chen *et al.*, 1987, 1990; Walker *et al.*, 1990; Bazett-Jones *et al.*, 1996). The three-dimensional DNA–phosphorus distribution reflects the unfolded nucleosome form, although it does not have the mass asymmetry of the entire DNA–protein particle. In contrast, the three-dimensional reconstructions of concomitantly purified nucleosomes in a transcriptionally quiescent chromatographic form, used as control, confirmed the closed compact nucleosome structure seen for transcriptionally inactive nucleosome particles in previous X-ray crystallographic and electron microscopic studies (Bentley *et al.*, 1984; Richmond *et al.*, 1984; Uberbacher and Bunick, 1989; Struck *et al.*, 1992; Arents and Moudrianakis, 1993; Czarnota and Ottensmeyer, 1996).

The unfolded form of the nucleosome is likely not an artifact of the preparation, but reflects an unfolding mechanism *in vivo* (Allegra *et al.*, 1987; Chen *et al.*, 1987, 1990; Walker *et al.*, 1990; Bazett-Jones *et al.*, 1996). Experiments have demonstrated that thiol accessibility correlates with gene expression in numerous systems. The chromatographic results accurately reflect tissue specificity of gene expression, cell cycle dependence of gene transcription, and the specific activation of gene expression following stimulation of cells with growth factors (Allegra *et al.*, 1987; Chen *et al.*, 1987, 1990; Walker *et al.*, 1990). Loss of binding activity also parallels the chemical inhibition of mRNA transcription and the down-regulation of genes (Chen *et al.*, 1990). The efficacy of the purification procedure has been demonstrated in numerous systems, including *Physarum* ribosomal RNA genes, nucleosomes from HeLa cells, and various mammalian tissues (Allegra *et al.*, 1987).

The three-dimensional DNA configuration within the nucleosome particle was observed in this study by the use of spectroscopic electron microscopy and difference image analysis methods. The generation of difference images which unequivocally represent the DNA phosphorus in an image of a nucleosome (Bazett-Jones and Ottensmeyer, 1981; Adamson-Sharpe and Ottensmeyer, 1981; Harauz and Ottensmeyer, 1984a; Locklear *et al.*, 1990; Oliva *et al.*, 1990; Czarnota and Ottensmeyer, 1996) is possible, since the signal from the DNA phosphorus is substantial. The scattering cross-section for phosphorus at 155 eV is at least 30 times greater than the cross-section for carbon at this energy (Heng *et al.*, 1990).

The DNA structure is consistent with a bent-spring model and nucleosome unfolding (Oliva *et al.*, 1987, 1990; Bazett-Jones *et al.*, 1996). The lobe-like appearance of the three-dimensional phosphorus map is commensurate with the 32 Å resolution of the reconstructions and very likely reflects the particle's conformational change that results in the elongated appearance. The lobe-like regions in the difference map were interpreted as unresolved elliptical loops formed by the double stranded DNA, upon analysis of their mass and after examination of 3D maps generated using different filtered backprojection schemes ranging from no filtering to full Shepp–Logan filtering and different display thresholds.

The structural differences between the quiescent and active chromatin subunits change the average physical parameters for the nucleosome particle in small but clearly significant ways. The 40.7 Å radius of gyration determined for the reconstruction of the nucleosome particles associated with actively transcribing genes was virtually identical to the 40.6 Å determined for highly acetylated particles in solution (Imai *et al.*, 1986). The value of 39.6 Å calculated for the reconstruction of transcriptionally quiescent particles was close to measured values of 39.1–40.9 Å determined using neutron diffraction (Pardon *et al.*, 1977; Suau *et al.*, 1977) and from a three-dimensional reconstruction of calf-thymus nucleosomes in a similar monovalent ionic environment (Czarnota and Ottensmeyer, 1996). Changes of a similar magnitude in radii of gyration have been found in previous determinations of nucleosome conformations (discussed in Czarnota and Ottensmeyer, 1996) in which a change from prolate to oblate conformation changed the radius of gyration from 37.9 to 39.1 Å. The correspondence between our values for the radii of gyration calculated from the 3D

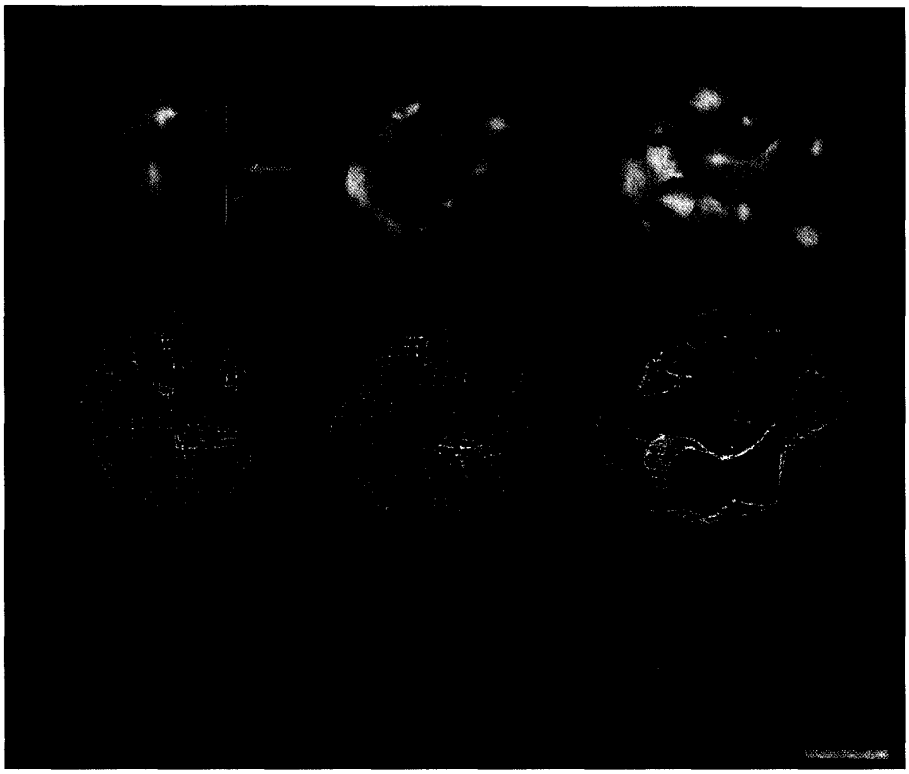

Fig. 6. Final nucleosome and difference-image-based three-dimensional reconstructions. The top row shows three views of the 155 eV energy loss reconstruction for the nucleosome particle at a contour which corresponds to the theoretical volume of combined protein and nucleic acid components of the nucleosome. The middle row shows the three-dimensional difference map fitted inside a wire-mesh representation of the 155 eV energy-loss nucleosome reconstruction. Over 95% of this map lies within the 155 eV reconstruction. In the bottom row the three-dimensional difference map is given alone. Each view from left to right is related to the previous one by a rotation of 45° towards the left about a vertical axis in the plane of the page. The 'L' indicates a slender phosphorus signal linker which joins two lobes of phosphorus signal denoted to the right by crosses, '+'. A 'C' indicates a cleft between the upper and lower domains of the structure. The scale bar indicates 50 Å.

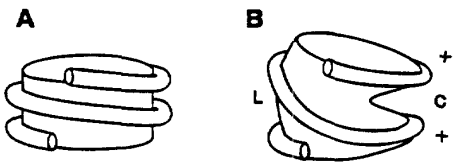

Fig. 7. A schematic representation of the changes in nucleosome structure based on three-dimensional reconstruction results of chromatographically purified particles. **A** represents the canonical conformation of the nucleosome associated with transcriptionally quiescent chromatin. **B** represents the C-shaped conformation of the nucleosome revealed by three-dimensional image reconstruction processes. The cleft between the upper and lower nucleosome domains is indicated by 'C'. The DNA in this type of particle in projection generates two lobes of phosphorus signal (marked to the right by crosses, '+') interpreted as distorted loop-like structures joined by a slender linker denoted by 'L'.

reconstructions and those measured from ensembles of nucleosomes in solution is reassuring. Although the changes in radii of gyration seem small compared to the rather obvious structural rearrangements of the nucleosome, they are consistent and clearly highly significant.

In this study the nucleosome particles purified from transcriptionally active chromatin had elevated levels of acetylation (Allegra *et al.*, 1987; Chen *et al.*, 1987, 1990; Oliva *et al.*, 1987, Walker *et al.*, 1990), a histone modification well correlated with gene expression and chromatin structure (van Holde, 1988; Turner, 1991; Felsenfeld, 1992; Grunstein *et al.*, 1992; Wolffe, 1994). Much experimental evidence has suggested that histone acetylation may unfold the nucleosome (reviewed in Oliva *et al.*, 1987, 1990). Compared to hypoacetylated nucleosome particles, highly acetylated particles exhibit differences in sedimentation coefficient (Ausio and van Holde, 1986), differences in thermal denaturation, fluorescence anisotropy and circular dichroism measurements (Bode *et al.*, 1980; Ausio and van Holde, 1986), differences in DNAseI sensitivity (Simpson, 1978; Ausio and van Holde, 1986), non-denaturing electrophoretic mobility (Bode *et al.*, 1980), and in protamine-mediated histone displacement (Oliva *et al.*, 1990). Nevertheless, some investigations detail only subtle changes in nucleosome conformation with acetylation. Nucleosomes without histone tails and hyperacetylated nucleosomes do not exhibit major changes in stability with respect to hypoacetylated particles (Ausio and van Holde, 1986; Ausio *et al.*, 1989). Additionally, acetylation alone does not increase the accessibility of histone H3 sulphydryls to chemical modifications, presenting the intriguing possibility that other factors may be involved

in changing the conformation of the nucleosome in association with active transcription (Boffa *et al.*, 1990; Marvin *et al.*, 1990). However, Norton *et al.* (1990a, 1990b) have detected a 20% reduction in the linking number change per nucleosome with histone H3 and H4 acetylation, and Bauer *et al.* (1994) present strong evidence that acetylation changes the shape of the histone octamer. In that investigation surface-linking theory demonstrated that a shape change consistent with data from hydroxy-radical footprinting experiments was associated with a decrease in the number of times DNA wound around the nucleosome central axis in acetylated particles. A change in shape towards a hyperboloid of revolution with histone acetylation was postulated to occur (Lee *et al.*, 1993). This shape change is consistent with some of the features of the nucleosome structure determined here if one considers rotating the particle about an axis perpendicular to the groove. A second model, the bipartite lexosome, based on physicochemical and biological experiments (Prior *et al.*, 1984), bears a striking resemblance to the two major lobes of the C-shaped view in the reconstructions.

As expected, the DNA trajectory determined from ESI microanalysis is consistent in projection with features seen in the two-dimensional phosphorus maps (Fig. 4). The observed distorted-spring trajectory would result in an increase in the average pitch of superhelical DNA winding about the nucleosomal central axis and can correlate with experimental evidence which suggests that positive supercoiling of DNA aids in the unfolding of nucleosome structure associated with gene expression (Norton *et al.*, 1990a, 1990b; Garcia-Ramiréz *et al.*, 1995). The increased accessibility of the nucleosome, as indicated by an open central core in the three-dimensional reconstructions of the particle and of its DNA–phosphorus trajectory, is also consistent with experiments which have shown an increased transcription factor access to DNA of acetylated nucleosomes (Lee *et al.*, 1993; Vetese-Dadey *et al.*, 1994, 1996). Moreover, the grossly different conformations of the nucleosomes from quiescent and from active chromatin, as indicated in this study, are consistent with previous investigations which have probed the structural dynamism of this chromatin subunit (Prior *et al.*, 1984; van Holde, 1988; Czarnota and Ottensmeyer, 1996).

Nucleosome structure is expected to be readily modifiable and dynamic since the particle represents a physical barrier to polymerase complexes which transcribe genes (van Holde, 1988; Turner, 1991; Felsenfeld, 1992; Grunstein *et al.*, 1992; Wolffe, 1994). The nucleosome particle has exhibited a dynamic nature as indicated by both genetic and biophysical studies (van Holde, 1988; Grunstein *et al.*, 1992; Czarnota and Ottensmeyer, 1996). Specifically, various ionic-strength-dependent and significantly different conformations of the nucleosome have been identified, indicating that charge-based interactions in principle should lead to changes in nucleosome configuration. Indeed, the core particle is stabilized by ionic interactions and exhibits several solvent-filled channels, which contribute towards stabilizing its structure (Arents and Moudrianakis, 1993). It has been argued (Lee *et al.*, 1993) that acetylation may alter such interactions and induce a disassociation between the DNA-wrapping globular domains of the histones and the adjacent DNA superhelix. Disassociation of the histone tails from DNA induced by changes in salt concentration has previously been demonstrated to be associated with an 'opening up' or disruption of nucleosome structure (Walker, 1984; Czarnota and Ottensmeyer, 1996).

A mass asymmetry has been observed previously in a preliminary investigation of gross particle conformation and interpreted as a disruption in nucleosome structure (Bazett-Jones *et al.*, 1996). This asymmetry is also reflected here in the three-dimensional reconstruction of the total particle. However, since the asymmetry is not found in the microanalytical determination of the DNA–phosphorus trajectory within the particle, it must be purely protein based. Mass analysis of the particles (Bazett-Jones *et al.*, 1996) indicates that adventitious proteins are not the cause of the observed mass asymmetry. The particles have the same integrated mass as the canonical transcriptionally inactive nucleosomes. Other investigations have demonstrated a mobility of H2A–H2B dimers in nucleosomes (Jackson, 1990) which could potentially contribute to the conformational changes revealed in this study.

The changes in nucleosome structure determined in this study may be elicited by the combinatorial effect of several biological processes. Recent investigations have determined an association between histone acetylation and transcriptional activity via nucleosome-linked SWI/SNF, RNA pol-II holoenzyme and histone acetyltransferase GCN5 as part of transcription activation (Hebbes *et al.*, 1988, 1994; Brownell *et al.*, 1996; reviewed in Wolffe and Pruss, 1996). Other studies have shown that hyperacetylation alone is not sufficient to elicit histone H3 sulphydryl accessibility, a defining feature of nucleosome particles associated with transcriptionally active chromatin (Marvin *et al.*, 1990; Boffa *et al.*, 1990). It is conceivable that nucleosome remodelling factors or transcriptional activators may be involved in processes which lead to acetylation-stabilized altered nucleosome structures associated with transcriptionally active chromatin (Peterson *et al.*, 1994; Peterson and Tamkun, 1995; Tsukiyama and Wu, 1995). More subtle changes in nucleosome structure have also been suggested between flanking regions and transcribed regions on active genes, one form of nucleosome being involved in transcriptional initiation and another facilitating elongation, respectively (van Holde *et al.*, 1992; Tazi and Bird, 1990).

Such structures are amenable to study by the currently demonstrated microanalytical and reconstruction approaches, but await refinements in biochemical purification techniques. For the present, the results presented here represent a powerful new combination of techniques in biochemistry, microanalysis and 3D reconstruction that has helped to elucidate the differences in structure between nucleosomes associated with

transcriptional quiescence and those participating in transcriptional activity. This study thus provides a structural basis and a technological foundation for future investigations aimed at the many perturbations in nucleosome structure which bear relevance to the processes of transcriptional control.

Acknowledgements—We thank Allan Fernandes and Yew Meng Heng for technical support and extend our gratitude to Dr George Harauz for the use of his IMAGIC image processing software. We thank Dr Michael J. Hendzel for his valuable comments on the manuscript. This work was supported by financial support to DPB-J and FPO from the Medical Research Council of Canada, and grants to FPO from the National Cancer Institute of Canada with funds from the Canadian Cancer Society, the Ontario Cancer Treatment and Research Foundation, and the National Sciences and Engineering Research Council of Canada. This work was also supported in part by a Steve Fonyo Fellowship from the NCIC to GJC, and an NIH research grant #CA-14908 to VGA. DPB-J was a scholar of the Alberta Heritage foundation for Medical Research.

REFERENCES

Adamson-Sharpe, K. M. and Ottensmeyer, F. P., 1981. Spatial resolution and detection sensitivity in microanalysis by electron loss selected imaging. *J. Microsc.*, **122,** 309–314.

Ahn, C. C., and Krivanek, O. L., 1983. *EELS Atlas*. Warrendale, PA.

Allegra, P., Sterner, R., Clayton, D. E. and Allfrey, V. G., 1987. Affinity chromatographic purification of nucleosomes containing transcriptionally active DNA sequences. *J. Mol. Biol.*, **196,** 379–388.

Andrews, D. W., Walter, P. and Ottensmeyer, F. P., 1987. Evidence for an extended 7SL RNA structure in the signal recognition particle. *EMBO J.*, **6,** 3471–3477.

Arents, G. and Moudrianakis, E. N., 1993. Topography of the histone octamer surface: repeating structural motifs utilized in the docking of nucleosomal DNA. *Proc. Natl Acad. Sci. USA*, **90,** 10489–10493.

Ausio, J. and van Holde, K. E., 1986. Histone hyperacetylation: its effects on nucleosome conformation and stability. *Biochemistry*, **25,** 1421–1428.

Ausio, J., Dong, F. and van Holde, K. E., 1989. Use of selectively trypsinized nucleosome core particles to analyze the role of the histone tails in the stabilization of the nucleosome. *J. Mol. Biol.*, **206,** 451–463.

Bauer, W. R., Hayes, J. J., White, J. H. and Wolffe, A. P., 1994. Nucleosome structural changes due to acetylation. *J. Mol. Biol.*, **236,** 685–690.

Bazett-Jones, D. P. and Brown, M. L., 1989. Electron microscopy reveals that transcription factor TFIIIA bends 5S DNA. *Mol. Cell. Biol.*, **9,** 336–341.

Bazett-Jones, D. P. and Ottensmeyer, F. P., 1981. Phosphorus distribution in the nucleosome. *Science*, **211,** 169–179.

Bazett-Jones, D. P., LeBlanc, B., Herfort. M. and Moss, T., 1994. Short-range looping by the Xenopus HMG-box transcription factor, xUBF. *Science*, **264,** 1134–1137.

Bazett-Jones, D. P., Mendez, E., Czarnota. G. J., Ottensmeyer, F. P. and Allfrey, V. G., 1996. Visualization and analysis of unfolded nucleosomes associated with transcribing chromatin. *Nuc. Acids Res.*, **24,** 321–329.

Beniac, D. R., Czarnota, G. J., Bartlett, T. A., Ottensmeyer, F. P. and Harauz, G., 1997a. Challenges of three-dimensional reconstruction of ribonucleoprotein complexes from electron spectroscopic images — reconstructing ribosomal RNA. *Scanning Microscopy Supplement: Proceedings of 15th Pfefferkorn Conference on Electron Image and Signal Processing*, ed. O. Johari (in press).

Beniac, D. R., Czarnota, G. J., Rutherford, B. L., Ottensmeyer, F. P. and Harauz, G., 1997b. Three-dimensional architecture of *Thermomyces langinosus* small subunit ribosomal RNA. *Micron*, **28,** 13–20. .

Beniac, D. R., Luckevich, M. D., Czarnota, G. J., Tompkins, T. A., Ridsdale, R. A., Ottensmeyer, F. P., Moscarello, M. A. and Harauz, G., 1997. Three-dimensional structure of myelin basic protein: reconstruction via angular reconstitution of randomly oriented single particles. *J. Biol. Chem.*, **272,** 4261–4268.

Bentley, G. A., Lewit-Bentley, A. L., Finch, J. T., Podjarny, A. D. and Roth, M., 1984. Crystal structure of the nucleosome core particle at 16 Å resolution. *J. Mol. Biol.*, **176,** 55–75.

Bertrand, E., Errand, M., Gómez-Lira, M. and Bode, J., 1984. Influence of histone hyperacetylation on nucleosome particles as visualized by electron microscopy. *Arch. Biochem. Biophys.*, **229,** 395–398.

Bode, J., 1984. Nucleosomal conformations induced by the small HMG proteins or by histone hyperacetylation are distinct. *Arch. Biochem. Biophys.*, **228,** 367–372.

Bode, J., Henco, K. and Wingender, E., 1980. Modulation of the nucleosome structure by histone acetylation. *Eur. J. Biochem.*, **110,** 143–152.

Bode, J., Gòmez-Lira, M. and Schröter, H., 1983. Nucleosome particles open as the histone core becomes hyperacetylated. *Eur. J. Biochem.*, **130,** 437–445.

Boffa, L. C., Walker, J., Chen, T. A., Sterner, R., Mariani, M. R. and Allfrey, V. G., 1990. Factors affecting nucleosome structure in transcriptionally active chromatin: histone acetylation, nascent RNA and inhibitors of RNA synthesis. *Eur. J. Biochem.*, **194,** 811–823.

Brownell, J. E., Zhou, J., Ranach, T., Kobayashi, R., Edmondson, D. G., Roth, S. Y. and Allis, C. D., 1996. Tetrahymena histone acetyltransferase A: a homolog to yeast GCN5P linking histone acetylation to gene activation. *Cell*, **84,** 843–851.

Cantor, C. R. and Schimmel, P. R., 1980. *Biophysical Chemistry*, pp. 608–633. W. H. Freeman, San Francisco, CA.

Chen, T. A., Smith, M. M., Le, S., Sternglanz, R. and Allfrey, V. G., 1987. Nucleosome fractionation by mercury affinity chromatography: contrasting distribution of transcriptionally active DNA sequences and acetylated histones in nucleosome fractions of the wild-type yeast cells and cells expressing a histone H3 altered to encode a cysteine 110 residue. *J. Biol. Chem.*, **266,** 6489–6498.

Chen, T. A., Sterner, R., Cozzolino, A. and Allfrey, V. G., 1990. Reversible and irreversible changes in nucleosome structure along the c-fos and c-myc oncogenes following inhibition of transcription. *J. Mol. Biol.*, **212,** 481–493.

Czarnota, G. J., 1995. Structural states of the nucleosome. PhD thesis, University of Toronto, p. 108.

Czarnota, G. J. and Ottensmeyer, F. P., 1996. Structural states of the nucleosome. *J. Biol. Chem.*, **271,** 3677–3683.

Czarnota, G. J., Andrews, D. W., Farrow, N. A. and Ottensmeyer, F. P., 1994. A structure for the signal sequence binding protein SRP54, 3D reconstruction from STEM images of single molecules. *J. Struct. Biol.*, **113,** 35–46.

Egerton, R. F., 1996. *Electron Energy-Loss Spectroscopy in the Electron Microscope*, pp. 216–219. Plenum Press, New York.

Farrow, N. A. and Ottensmeyer, F. P., 1992. *A posteriori* determination of relative projection directions of arbitrarily oriented macromolecules. *J. Opt. Soc. Am.*, **A9,** 1749–1760.

Farrow, N. A. and Ottensmeyer, F. P., 1993. Automatic 3D alignment of projection images of randomly oriented objects. *Ultramicroscopy*, **52,** 141–156.

Felsenfeld, G., 1992. Chromatin as an essential part of the transcriptional mechanism. *Nature*, **255,** 219–224.

Fiori, C. E., Leapman, R. D., Swyt, C. R. and Andrews, S. B., 1988. Quantitative X-ray mapping of biological sections. *Ultramicroscopy*, **24,** 237–250.

Garcia-Ramiréz, M., Rocchini, C. and Ausio, J., 1995. Modulation of chromatin folding by histone acetylation. *J. Biol. Chem.*, **270,** 17923–17928.

Grunstein, M., Durrin, L. K., Mann, R. K., Fisher-Adams, G. and Johnson, L. M., 1992. Histones: regulators of transcription in yeast. In *Transcriptional Regulation*, ed. S. L. McKnight and K. R. Yamamoto, pp. 1295–1315. Cold Spring Harbor Laboratory, Cold Spring Harbor, NY.

Harauz, G., 1990. Representation of rotations by unit quaternions. *Ultramicroscopy*, **33,** 209–213.

Harauz, G. and Ottensmeyer, F. P., 1984. Nucleosome reconstruction via phosphorus mapping. *Science*, **226,** 936–940.

Harauz, G. and Ottensmeyer, F. P., 1984. Direct three-dimensional reconstruction for macromolecular complexes from electron micrographs. *Ultramicroscopy*, **12,** 309–320.

Harauz, G., Czarnota, G. J., Cejka, Z., Ciciopol, C., Hegere, R., Typke, D., Ottensmeyer, F. P. and Baumeister, W., 1998. Three-dimensional cryoelectron microscopic reconstruction of the

2.25 MDa homomultimeric phosphoenolpyruvate synthase from *Staphylothermus marinus*. Submitted.

Hebbes, T. R., Thorne, A. W. and Crane-Robinson, C., 1988. A direct link between core histone acetylation and transcriptionally active chromatin. *EMBO J.*, **7,** 1395–1402.

Hebbes, T. R., Clayton, A. L., Thorne, A. W. and Crane-Robinson, C., 1994. Core histone hyperacetylation co-maps with generalized DNaseI sensitivity in the chicken beta-globin chromosomal domain. *EMBO J.*, **13,** 1823–1830.

Heng, Y. M., Simon, G. T., Boublik, M. and Ottensmeyer, F. P., 1990. Experimental ionization cross-sections of phosphorus and calcium by electron spectroscopic imaging. *J. Microsc.*, **160,** 161–171.

Imai, B. S., Yau, P., Baldwin, J. B., Ibel, K., May. R. P. and Bradbury, E. M., 1986. Hyperacetylation of core histones does not cause unfolding of nucleosomes, neutron scatter data accords with disc shape of the nucleosome. *J. Biol. Chem.*, **261,** 8784–8792.

Jackson, V., 1990. *In vivo* studies on the dynamics of histone–DNA interactions: evidence for nucleosome dissolution during replication and transcription and a low level of dissociation independent of both. *Biochemistry*, **29,** 719–731.

Lee, D. Y., Hayes, J. J., Pruss, D. and Wolffe, A. P., 1993. A positive role for histone acetylation in transcription factor access to nucleosomal DNA. *Cell*, **72,** 73–84.

LeFurgey, A., Davilla, S. D., Kopf, D. A., Sommer, J. R. and Ingram, P., 1992. Real-time quantitative elemental analysis and mapping: microanalytical imaging in cell physiology. *J. Microscopy*, **165,** 191–223.

Locklear, L. Jr, Ridsdale, J. A., Bazett-Jones, D. P. and Davie, J. R., 1990. Ultrastructure of transcriptionally competent chromatin. *Nuc. Acids Res.*, **18,** 7015–7024.

Marvin, K. W., Yau, P. and Bradbury, E. M., 1990. Isolation and characterization of acetylated histones H3 and H4 and their assembly into nucleosomes. *J. Biol. Chem.*, **265,** 19839–19847.

Neil, K. J., Ridsdale, R., Rutherford, B., Taylor, L., Larson, D. E., Gilbeitic, M., Rothblum, L. I. and Harauz, G., 1996. Structure of recombinant rat UBF by electron image analysis and homology modelling. *Nuc. Acids. Res.*, **24,** 1472–1480.

Norton, V. G., Imai, B. S., Yau, P. and Bradbury, E. M., 1990. Histone acetylation reduced nucleosome core particle linking number. *Cell*, **57,** 449–457.

Norton, V. G., Marvin, K. W., Yau, P. and Bradbury, E. M., 1990. Nucleosome linking number change controlled by acetylation of histones H3 and H4. *J. Biol. Chem.*, **265,** 19848–19852.

Oliva, R., Bazett-Jones, D. P., Mezquita, C. and Dixon, G., 1987. Factors affecting nucleosome disassembly by protamines *in vitro*: histone hyperacetylation and chromatin structure, time dependence, and the size of the sperm nuclear proteins. *J. Biol. Chem.*, **262,** 17016–17025.

Oliva, R., Bazett-Jones, D. P., Locklear, L. Jr, Dixon, G. H., 1990. Histone hyperacetylation can induce unfolding of the nucleosome core particle. *Nuc. Acids Res.*, **18,** 2739–2747.

Pardon, J. F., Worcester, D. L., Wooley, J. C., Cotter, R. I., Lilley, D. M. J. and Richards, B. W., 1977. The structure of the chromatin core-particle in solution. *Nucleic Acids Res.*, **4,** 3199–3214.

Peterson, C. L. and Tamkun, J. W., 1995. The SWI–SNF complex: a chromatin modelling machine. *Trends. Biochem. Sci.*, **20,** 143–146.

Peterson, C. L., Dingwall, A. and Scott, M. P., 1994. Five SWI/SNF gene products are components of a large multisubunit complex required for transcriptional enhancement. *Proc. Natl Acad. Sci. USA*, **91,** 2905–2908.

Prior, C., Cantor, C. R., Johnson, E. M., Littau, V. C. and Allfrey, V. G., 1984. Reversible changes in nucleosome structure and histone H3 accessibility in transcriptionally active and inactive states of rDNA chromatin. *Cell*, **34,** 1033–1042.

Richmond, T. J., Finch, J. T., Rushton, B., Rhodes, D. and Klug, A., 1984. Structure of the nucleosome core at 7 Å resolution. *Nature*, **311,** 532–537.

Rose, A., 1973. *Vision: Human and Electronic*. Plenum Press, New York.

Shepp, L. A. and Logan, B. F., 1974. The Fourier reconstruction of a head section. *I.E.E.E. Trans. Nucl. Sci.*, **WS-21,** 21–43.

Simpson, R. T., 1978. Structure of chromatin containing extensively acetylated H3 and H4. *Cell*, **13,** 691–699.

Somlyo, A. V., Shuman, H. and Somlyo, A. P., 1981. Electron probe analysis of cardiac, skeletal, and vascular smooth muscle. In *Microprobe Analysis of Biological Systems*, ed. T. E. Hutchison and A. P. Somlyo, pp. 103–126. Academic Press, New York.

Struck, M. M., Klug, A. and Richmond, F. J., 1992. Comparison of X-ray structures of the nucleosome core particle in two different hydration states. *J. Mol. Biol.*, **224,** 253–264.

Suau, P., Kneale, G. G., Braddock, G. W., Baldwin, J. P. and Bradbury, E. M., 1977. A low resolution model for the chromatin core particle by neutron scattering. *Nuc. Acids Res.*, **4,** 3199–3214.

Tazi, J. and Bird, A., 1990. Alternative chromatin structure at CpG islands. *Cell*, **60,** 909–920.

Tsukiyama, T. and Wu, C., 1995. Purification and properties of an ATP-dependent nucleosome remodelling factor. *Cell*, **83,** 1011–1020.

Turner, B. M., 1991. Histone acetylation and control of gene expression. *J. Cell. Sci.*, **99,** 13–20.

Uberbacher, E. C. and Bunick, G. J., 1989. Structure of the nucleosome core particle at 8 Å resolution. *J. Biomol. Struct. Dyn.*, **7,** 1033–1055.

Vainshtein, B. K. and Goncharov, A. B., 1986. Determination of the spatial orientation of arbitrarily arranged identical particles of an unknown structure from their projections. *Proceedings of the XIth International Congress on Electron Microscopy*, Kyoto, Japan, pp. 459–460.

van Heel, M., 1987. Angular reconstitution, *a posteriori* assignment of projection directions for 3D reconstruction. *Ultramicroscopy*, **21,** 111–124.

van Heel, M. and Harauz, G., 1986. Resolution criteria for three-dimensional reconstruction. *Optik*, **73,** 119–122.

van Holde, K. E., 1988. *Chromatin*. Springer-Verlag, New York.

van Holde, K. E., Lohr, D. E. and Robert, C., 1992. What happens to nucleosomes during transcription? *J. Biol. Chem.*, **262,** 17016–17025.

Vettese-Dadey, M., Walter, P., Chen, H., Juan, L. J. and Workman, J. L., 1994. Role of the histone amino termini in facilitated binding of a transcription factor, GAL4-AH, to nucleosome cores. *Mol. Cell. Biol.*, **14,** 970–981.

Vettese-Dadey, M., Grant, P. A., Hebbes, T. R., Crane-Robinson, C., Allis, C. D. and Workman, J. L., 1996. Acetylation of histone H4 plays a primary role in enhancing transcription factor binding to nucleosomal DNA *in vitro*. *EMBO J.*, **15,** 2508–2518.

Walker, I. O., 1984. Differential dissociation of histone tails from core chromatin. *Biochemistry*, **23,** 5622–5628.

Walker, J., Chen, T. A., Sterner, R., Berger, M., Winston, F. and Allfrey, V. G., 1990. Affinity chromatography of mammalian and yeast chromosomes: two modes of binding of transcriptionally active nucleosomes to organomercurial–agarose columns, and contrasting behaviour of the active nucleosomes of yeast. *J. Biol. Chem.*, **265,** 5736–5746.

Wolffe, A., 1994. Transcription, in tune with the histones. *Cell*, **77,** 13–16.

Wolffe, A. P. and Pruss, D., 1996. Targeting chromatin disruption: transcription regulators that acetylate histones. *Cell*, **84,** 817–819.

Zabal, M. M., Czarnota, G. J., Bazett-Jones, D. P. and Ottensmeyer, F. P., 1993. Characterization of nucleosomes from their electron micrographs by principal component analysis. *J. Microscopy*, **172,** 205–214